



Interaction of silver nanoparticles with an environmentally beneficial bacterium, *Pseudomonas chlororaphis*

Christian O. Dimkpa^{a,*}, Alyssa Calder^a, Priyanka Gajjar^a, Srinivas Merugu^b, Wenjie Huang^c, David W. Britt^a, Joan E. McLean^d, William P. Johnson^b, Anne J. Anderson^{e,a}

^a Department of Biological Engineering, Utah State University, Logan, UT 84322, USA

^b Geology and Geophysics, University of Utah, Salt Lake City, UT 84112, USA

^c Chemical Engineering, University of Utah, Salt Lake City, UT 84112, USA

^d Utah Water Research Laboratory, Utah State University, Logan, UT 84322, USA

^e Department of Biology, Utah State University, Logan, UT 84322 USA

ARTICLE INFO

Article history:

Received 20 October 2010

Received in revised form 27 January 2011

Accepted 31 January 2011

Available online 20 February 2011

Keywords:

Extracellular polymeric substance

Pseudomonas chlororaphis

Reactive oxygen species

Silver ion

Silver nanoparticles

Toxicity

ABSTRACT

This study explores the potential antimicrobial mechanisms of commercial silver nanoparticles (Ag NPs) in the environmental bacterium, *Pseudomonas chlororaphis* O6. The 10 nm size NPs aggregated in water, as demonstrated by atomic force microscopy. Solubility of the NPs at 10 mg/L was 0.28 mg/L (pH 6) and 2.3 mg/L (pH 7); release from 10 mg/L bulk Ag was below detection. The NPs eliminated cell culturability at 3 mg/L, whereas no effect was observed at 10 mg/L bulk Ag. Zeta potential measurements revealed that the NPs were negatively charged; unlike Ag ions, their addition to the negatively charged cells did not change cell charge at pH 6, but showed a trend to reduce cell charge at pH 7. Isolated extracellular polymeric substances (EPS) from PcO6 was polydisperse, with negative charge that was neutralized by Ag ions, but not by the NPs. Addition of EPS eliminated Ag NP's toxicity in cells lacking EPS. Intracellular accumulation of $\cdot\text{OH}$ was not detected in NP-treated cells; however, the use of scavengers suggested the NPs caused extracellular H_2O_2 production. No evidence was found for loss of membrane integrity upon treatment with the NPs. Our findings indicate that growth of environmental bacteria could be impaired by Ag NPs, depending on the extent of EPS production.

© 2011 Elsevier B.V. All rights reserved.

1. Introduction

Silver (Ag) nanoparticles (NPs) are deployed in many applications, including water purification, antifouling surfaces, and aseptic food packaging because of their antimicrobial potential. Medical applications include wound dressings, surface sterilization of devices and implantations, masks, clothing, and bedding [1,2]. The increasing resistance of pathogenic bacteria to traditional antibiotics makes Ag NPs useful alternative antimicrobial agents.

Dose-dependent antimicrobial effects of Ag NPs are reported for pathogens such as *Escherichia coli* and *Staphylococcus aureus*. Efficacy is dependent on bacterial strain and on properties of the NPs endowed by their method of synthesis [3–6]. Size and shape are important, with micro-scale particles (“bulk” equivalent) showing lesser effects than the NPs [4,7–11]. The release of Ag ions from Ag NPs participates in their antimicrobial activity [12–15], thus extending the historical use of Ag ions as an antimicrobial agent. Ag NPs effect cell membranes [10], electron transport

[16] and ATP-dependent transport mechanisms in bacterial cells [17].

The widespread use of Ag NPs raises the question of the ecological risk associated with increased Ag contamination of the environment [18]. The Ag NPs display antimicrobial activity against environmental *Pseudomonas* isolates [3,4], and they disturb biofilm integrity [19]. In this paper we focus on better understanding of the mechanisms of interaction between Ag NPs and a beneficial soil pseudomonad, *Pseudomonas chlororaphis* O6 (PcO6). Root colonization by PcO6 promotes plant growth and tolerance to abiotic and pathogen stresses [20,21]. Bacterial extracellular polymeric substance (EPS) enveloping the cells could act as a protective material against environmental stressors including NPs [18,22]. We investigated the surface interactions between Ag NPs, cells, and EPS produced by the cells using zeta (ζ) potential measurements. Fast flow fractionation (FFF), a powerful tool for studying particle size in suspensions [4], and atomic force microscopy (AFM) for direct imaging, were used to determine size distribution of the Ag NPs and the particles in EPS. Increases in reactive oxygen species (ROS) is a proposed cause of Ag toxicity [10,13,23–27]. Consequently, we examined the ability of Ag NPs to stimulate extra- and intra-cellular reactive oxygen species production in PcO6 cells. We used 3'-

* Corresponding author. Tel.: +1 435 7973497.

E-mail address: cdimkpa@usu.edu (C.O. Dimkpa).

(*p*-aminophenyl) fluorescein (APF) and dichlorodihydrofluorescein diacetate (H_2 -DCFDA) as indicators of intracellular accumulation of hydroxyl radicals in Gram-negative bacteria [7]. The effect of the NP treatments on membrane integrity was studied by following the release of the periplasmic marker enzyme, alkaline phosphatase, or green fluorescent protein expressed in the cytoplasm of reporter cells. Previous studies with a pseudomonad biosensor in *P. putida* strain KT2440 showed that cellular toxicity occurred at similar levels of metal (0.2–0.3 mg Ag/L) from the ions or the Ag NPs [4]. Therefore, where appropriate, studies were included to compare the effect of Ag ions and bulk Ag to that of the Ag NPs.

2. Experimental

2.1. Sources of Ag

A commercial Ag NP suspension in water was obtained from ATTOSTAT Inc. (West Jordan, UT, USA). The Ag NP has an as-made size of 10 nm, at a concentration of 22.4 mg/L. The NPs have no surface coatings and were made by a laser-based technology. Ag ions from $AgNO_3$ and bulk Ag (44,000 nm) were obtained from Alfa Aesar (MA, USA). Sterile deionized distilled water was used in all studies.

2.2. Bacterial strain and growth conditions

PcO6 cells were stored in 15% glycerol at $-80^\circ C$ before use. The cells were cultured in a minimal salts medium (MM) with sucrose and citrate as the carbon sources as described by Gajjar et al. [4]. Cells were grown overnight, transferred to a new MM, and grown to log phase ($OD_{600\text{ nm}} = 0.1$). Cells were obtained as a pellet by centrifugation ($10,000 \times g$ for 10 min at RT) and resuspended in the same volume of sterile, distilled deionized water, to give an initial cell count of 10^8 culturable cells/mL. This suspension was used in the studies described below. Cell culturability was determined by dilution plating in sterile water onto Luria Broth (LB) agar medium, and counting colonies after 48–72 h of incubation at $26^\circ C$.

2.3. Characterization of the Ag NPs and cell interactions with NPs

2.3.1. Zeta (ζ) potential measurements

The surface charge of the Ag NPs was examined using a Zeta Meter (Zeta Meter Inc., VA, USA). Suspensions of PcO6 cells were treated with 1.5 and 10 mg/L Ag as Ag NPs or ions for 60 min with shaking at 200 rpm at $26^\circ C$; control suspensions lacked any amendments. To evaluate the effect of pH, these suspensions were adjusted to pH 6 and 7 using 0.5 M KOH or 0.5 N HCl.

2.3.2. Atomic force microscopy of nanoparticles, cells and EPS

A Nanoscope III Bioscope (Digital Instruments, Inc.) was used in tapping mode to image the Ag NPs, cells and EPS suspensions evaporated from water on freshly cleaved muskovite mica. The samples were applied in a 10 μ L volume. Images were collected at multiple size scales and scan angles to help account for any tip induced artifact. MikroMasch Ultrasharp CSC12 uncoated cantilevers with tip radius of curvature less than 10 nm that were 250 μ m long, 35 μ m wide, 1.0 μ m thick with nominal force constants of 0.08 N/m were employed. To avoid sweeping of the samples by the AFM tip, scan rates between 1 and 14 Hz were employed. The tip-sample force was reduced to the minimal value by adjusting the set point voltage until the tip came out of contact, then entering a value to bring the tip just back into contact. For the bulk Ag powder, 10 μ L of the suspension (10 mg/L) in water was evaporated on glass slides and imaged with a NIKON Eclipse TE2000-S light microscope.

2.3.3. Fast flow fractionation of Ag NPs

FFF of the Ag NPs was performed to obtain information on size of the particles. An asymmetric flow field flow fractometer (AF2000, Postnova, Inc., Salt Lake City, UT) was used with an online UV detector (FFF-UV) and FL27 in the carrier solution contained [4]. Fractionations were calibrated using gold (10 nm particles) and fluorescent latex beads (98 and 200 nm).

2.3.4. Evaluation of solubility of Ag NPs and bulk Ag

The Ag NP or bulk Ag stock suspension was diluted to 10 mg/L in water, adjusted to pH 6 or 7, shaken gently for 60 min and then centrifuged at $15,557 \times g$ for 30 min. The supernatant was removed with care and recentrifuged. This second supernatant was assayed for soluble Ag contents by inductively coupled plasma mass spectrometry (ICP-MS).

2.4. EPS studies

EPS was extracted from PcO6 cells grown on BSM plates supplemented with 2% (v/v) glycerol instead of sucrose as the carbon source for 4 d at $26^\circ C$. The cells were scraped from the surface and suspended in sterile 0.9% (w/v) NaCl. The suspension was stirred vigorously with glass beads (200 rpm) for 1 h to detach the EPS associated with cells, thereby generating EPS-deficient cells. Cells were pelleted by centrifugation ($10,000 \times g$; 30 min), and the resultant supernatant was treated twice with 95% ethanol at $4^\circ C$. After standing for 2 h, the precipitate was recovered by centrifugation. The pellets were suspended in sterile distilled deionized water and the concentration of neutral sugars was determined by the Dubois colorimetric method [28]. The EPS preparations were frozen until used. The ζ -potential of the EPS, with and without mixing with NPs and ions, was determined as described above. FFF was performed to determine EPS particle size using UV detection and Milli-Q water as carrier.

2.5. Effect of EPS on cell culturability after Ag NPs and Ag ions treatments

Suspensions of cells with and without EPS, prepared as described above, were amended with defined concentrations of Ag NPs or Ag ions for 60 min with shaking at 200 rpm at $26^\circ C$. Control cells had no metal amendments. Cell suspensions were serially diluted and aliquots plated on LB agar to determine culturability.

2.6. Assessment of ROS generation from Ag NPs

2.6.1. Use of the intracellular fluorescent dyes APF and H_2 -DCFDA

The cells in water suspension were treated with defined concentrations of Ag NPs or ions (0, 0.2, 0.5, 1.0 and 1.5 mg/L) and were incubated for 60 min in light. Three replicated aliquots (100 μ L) were dispensed into 96-well plates, and APF (Invitrogen, OR, USA), was added to a final dye concentration of 5 μ M in a final volume of 200 μ L. Samples were maintained in darkness, and fluorescence readings were immediately taken at 485 nm for excitation and 535 nm for emission (Synergy4 Hybrid Multi-Mode Microplate Reader, BioTek, Inc., VT, USA). Plates were subsequently incubated for 20 min to permit penetration of the dye into the cell [7]. Incubation was at room temperature and under normal laboratory lighting. The fluorescence of the samples was again recorded and the difference between the two readings calculated. For each treatment there were three replicated fluorescent measurements. Two separate studies were performed. A second fluorescence dye H_2 -DCFDA also with specificity for hydroxyl radicals (Invitrogen, USA) was used [7]. Cells in MM were treated with 10 μ M of the dye, incubated in the dark for 30 min, and then pelleted by centrifugation. The cell pellet was resuspended with and without amendments of

0.2 and 1.5 mg/L NPs or ions and incubated for 20 min in the dark, after which fluorescence was measured at 485 nm excitation and 535 nm emission filters [7].

2.6.2. Use of ROS scavengers

Cell suspensions (2 mL) were treated with 1.5 mg/L of Ag NPs or ions for 60 min in the presence or absence of catalase (CAT; 286 units, Sigma, MO, USA) to degrade H₂O₂, superoxide dismutase (SOD; 200 units Sigma, MO, USA) to degrade superoxide anion, or 0.3 M methanol to scavenge ROS [12,22]. Cell culturability was determined by dilution plating onto LB agar medium. Control assays were performed with the same aliquots of heat-denatured enzymes to demonstrate that protection was due to enzyme activities and not just the presence of protein. Denaturation was achieved by boiling the enzymes in water for 20 min.

2.7. Evaluation of effect of Ag NPs on membrane integrity

To examine the possible effects of the NPs on the integrity of the outer membrane of the bacterial cell, the release of a periplasmic enzyme, alkaline phosphatase (Alp), was monitored. Cells suspensions, with and without treatment by Ag NPs and Ag ions for 30 min, were centrifuged, and the pelleted cells resuspended in 5 mM Ca(NO₃)₂ for 15 min with slow shaking (80 rpm) to allow for cation exchange at the cell surface [29]. The suspensions were centrifuged and both pellet and supernatant were saved. The pelleted cells were suspended in 15 mL 20 mM EDTA (tetra sodium salt; pH 9.76) for 20 s to disrupt the outer membrane and, release periplasmic contents [29]. The supernatants from both Ca- and EDTA-treatments were assayed for alkaline phosphatase (Alp) activity using 1 mM para-nitrophenol phosphate (P-NPP) as the substrate [30] in 20 mM Ca added to chelate the EDTA. Formation of para-nitrophenol (PNP) at pH 8.5 was measured at 410 nm. To test the direct effect of ions or NPs on Alp activity, the enzyme was released from control cells by EDTA lysis to obtain the periplasmic fraction. The enzyme in the extract was exposed to ions or NPs for 30 min before comparing Alp activity to that in a control lacking metal treatments.

Plasma membrane integrity in the presence of the Ag NPs and ions was evaluated by screening for loss of green fluorescent protein (GFP) from cells of *PcO6* engineered to express (GFP) in the cytoplasm. The cells were generated through transfer of a plasmid containing the *gfp* gene following the procedures described by Kim et al. [31]. Expression of the protein was verified by microscopy of intact cells on a Nikon TE2000 microscope. Release of GFP was studied with suspensions of the logarithmic phase cells suspended at 10⁸ cells/mL in sterile distilled water or with 10 mg/L Ag NPs or ions. Cells suspensions were shaken gently for 60 min were pelleted by centrifugation to obtain the cell-free supernatants. For lysis, the cells were suspended in 30 mM Tris-HCl buffer (pH 8), and 20 μL/mL of lysozyme (Fisher Bioreagents BP534-1) was added for a 30 min treatment. The reaction mixture was centrifuged at 10,000 × g for 10 min. The fluorescence of the supernatants was examined in a RF-1501-Shimadzu fluorometer with an excitation wavelength of 488 nm and emission wavelength of 509 nm. The study was repeated three times, and the fluorescence of each of the supernatants was read in duplicate.

3. Results

3.1. Characterization of the Ag NPs

The commercial Ag NPs are spherical with a particle size of 10 nm (TEM information supplied by manufacturer; Fig. 1A). Our AFM analysis confirmed the existence of particles with this dimension (Fig. 1B). However, AFM imaging also showed that the water

suspended preparations contained agglomerates in the micron-size range (Fig. 1C). Microscopy of the bulk Ag showed amorphous micron-sized particles visible in the light microscope with very irregular surfaces (Fig. 1D). FFF characterization of the Ag NPs suspension further confirmed the presence of particles of 10 nm size but larger masses of 70–90 nm (Fig. 2A). At 1.5 mg/L Ag NPs did not produce enough particles for reliable ζ-potential measurements (data not shown). However, the preparation of 10 mg/L Ag NPs had visible particles with negative charges, –33 mV at pH 6 and –35 mV at pH 7. Analysis of solubilized metal showed 0.28 mg/L Ag was released at pH 6 and 2.3 mg/L at pH 7 from a stock of 10 mg/L Ag NPs. Solubility from a 10 mg/L suspension of bulk Ag was below detection at both pH 6 and 7.

3.2. Interactions with *PcO6* cells: surface charge effects

ζ-potential measurements revealed that *PcO6* cells possessed a negative surface charge that was more negative at pH 7 than at pH 6. Addition of the Ag NPs had no effect on cell charge at pH 6; at pH 7 however, there was a trend for reduced negative charge. Negative charge was significantly reduced ($P < 0.05$) by addition of 10 mg/L Ag ion at pH 7 (Fig. 3).

To test whether EPS might contribute to the negative charge of the cells, EPS was extracted from *PcO6*. Polydispersity of the EPS was evident by AFM imaging (Fig. 1G). Similarly FFF analysis showed particles to peak in size at about 10 μm (Fig. 2B). The EPS preparations contained neutral sugars (stock solutions equivalent to 1.62 g glucose/L). ζ-potential measurements showed negatively charged particles with values only slightly lower than those of intact cells. Mixing the EPS (1.4 g/L final concentration) with Ag NPs did not change the charge whereas Ag ions reduced the net negative charge at both pH 6 and 7 (Fig. 3). AFM imaging was unable to distinguish particles of Ag NPs from those of the EPS in EPS-Ag NP mixtures (Fig. 1G versus H).

3.3. Effect of Ag NPs on cell culturability

Ag NPs caused dose-dependent loss in cell culturability, with 3 mg/L being lethal. Fig. 1F shows an AFM image of cells associated with agglomerated Ag NPs, a dose that reduced culturability from 10⁸ to 10⁴ cells/mL. The AFM imaging did not show Ag NPs associated with flagella and the wall structure of the bacteria appeared intact (Fig. 1F). Delay in colony formation from 24 to 72 h on the LB plate medium occurred after the treatments for 60 min with 1.5 and 2 mg/L Ag NPs, and 1 mg/L Ag ion treatments. Ag ions at 1.5 mg/L eliminated culturability (Fig. 4). The pH of the suspensions for these treatments was similar (pH 7.06 ± 0.06). Contrary to both Ag NP and Ag ions, exposure of cells for 60 min to bulk Ag up to 10 mg Ag/L had no effect on cell growth (Fig. 4).

3.4. Protective effect of EPS against Ag NPs

Addition of extracted EPS (0.8 g glucose equivalents/L) to the *PcO6* cells did not alter the culturability of normal cells or cells from which EPS had been removed (Figs. 1I and 5). Cells rendered deficient in EPS were completely inactivated by Ag NPs at 1.5 mg/L, while the control cells with the normal EPS layer showed only reduced culturability. The addition of EPS increased the culturability of both cell types in the presence of the NPs and Ag ions (Fig. 5). No protection was observed by EPS at treatments of 10 mg/L of Ag NPs. AFM images of the *PcO6* cells in the mixtures with EPS and Ag NPs showed the presence of intact cells (Fig. 1J).

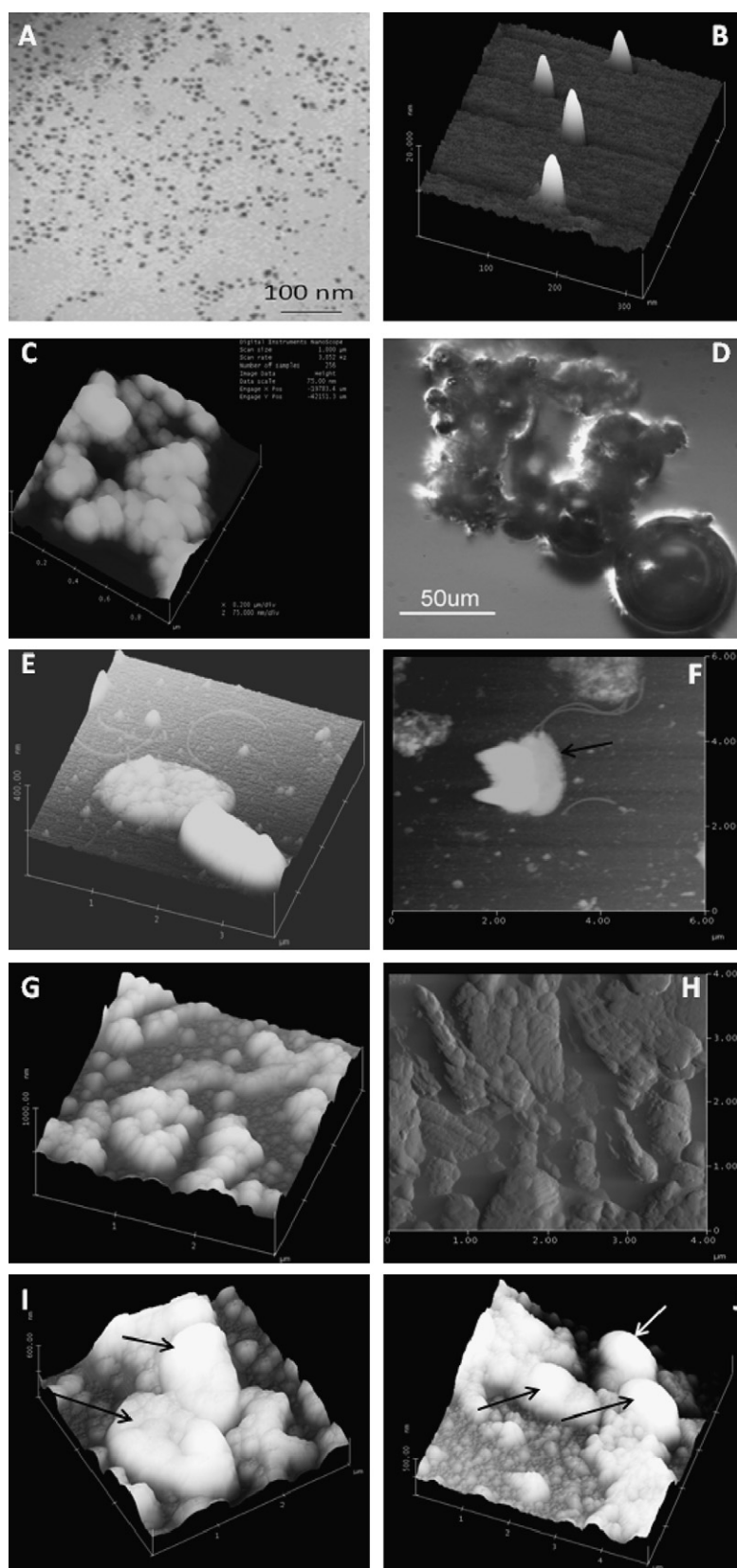


Fig. 1. (A) Transmission electron microscopy image of ATTOSTAT Ag NPs as supplied by the manufacturer, indicating monodispersed spherical 10 nm particles. Representative atomic force microscopy (AFM) images of (B) ATTOSTAT Ag NPs showing single NPs with a vertical dimension of about 10 nm (C) ATTOSTAT Ag NPs in submicron agglomerates. (D) Light microscopy of bulk Ag from water suspension (E) AFM of cells of *Pco6* from a water suspension; detached flagella are visible. (F) AFM of *Pco6* cells in water suspension amended with 1.5 mg/L Ag NPs; an agglomerate of Ag NPs is associated with the cell surface (cell noted by arrow). (G) AFM of extracellular polymeric substances (EPS) extracted from *Pco6* showing sub micron to micron-sized particles. (H) AFM of a mixture of EPS and ATTOSTAT Ag NP (1.5 mg/L); the Ag NP aggregates cannot be resolved from the polydispersed EPS material. (I) AFM of *Pco6* cells in a suspension of EPS; cells (arrowed) are present in the EPS polymeric background. (J) AFM of a mixture of *Pco6* cells, ATTOSTAT Ag NP (1.5 mg/L) and EPS; cells (arrowed) are seen within the polymeric mixture.

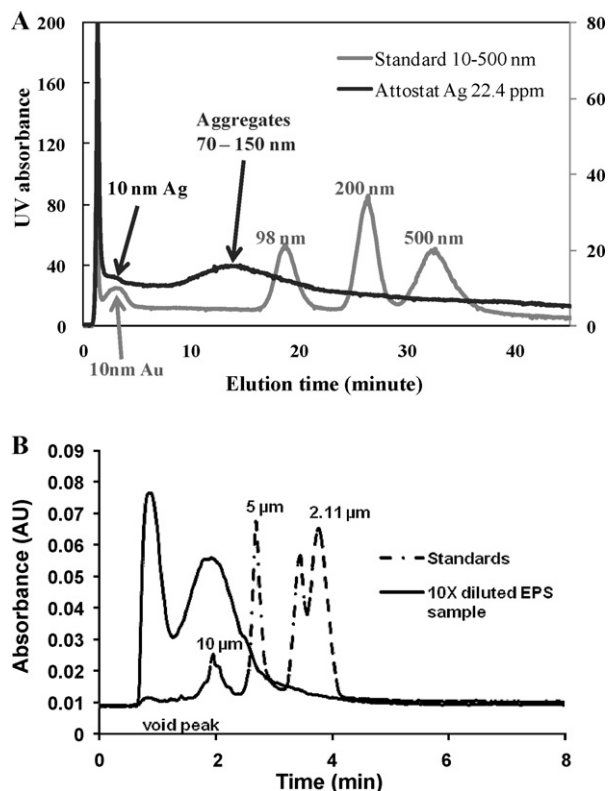


Fig. 2. (A) Fast flow fractionation (FFF)-UV fractogram of ATTOSTAT Ag NPs showing particles in the 10 nm size and aggregates of 70–150 nm and (B) FFF-UV fractogram of a 10 \times -diluted EPS sample demonstrating the presence of micron-sized particles. Fractionation of standard particles is shown for both fractograms. AU=arbitrary unit.

3.5. Detection of reactive oxygen species in Ag NP-challenged cells

Whereas treatment with 1.5 mg/L Ag NPs reduced culturability from 10^8 to 10^4 cfu/mL, exposure of cells for 20 min to between 0.2 and 1.5 mg/L Ag NPs under room lighting did not stimulate intracellular accumulations of hydroxyl radicals as detectable with APF (Fig. 6A). However, APF fluorescence increased with treatments of 1 (change in culturability from 10^8 to 10^4 cfu/mL) and 1.5 mg/L Ag ions (complete loss in culturability). No differences in fluorescence were observed between assays performed in darkness and those performed in laboratory lighting, suggesting that photocatalysis was not involved in generation of the ROS (data not shown). A second dye, H_2 -DCFDA, which also responds to hydroxyl radicals, gave similar results as APF, except that there was no change in fluorescence for the Ag ion exposure (Fig. 6B).

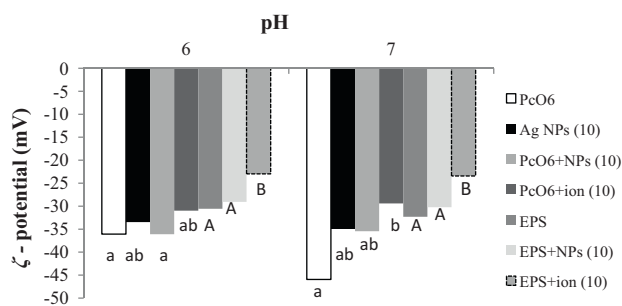


Fig. 3. ζ -potential measurement of PcO6 cells (OD 600 nm = 0.1) and EPS extracted from PcO6, suspended in water with or without Ag NPs and Ag ions (10 = 10 mg/L). Different letters in bars indicate significant differences within each pH value (where $P < 0.05$) for cells (lower case) and EPS (upper case).

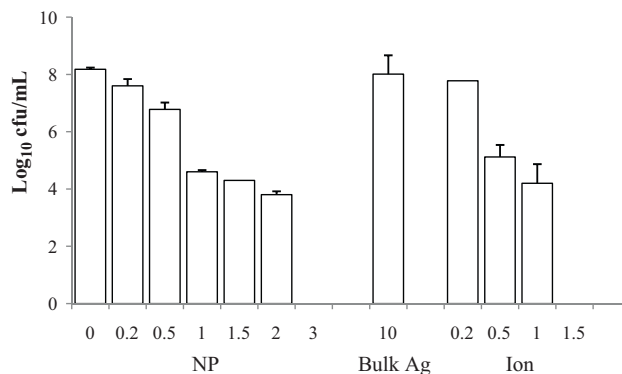


Fig. 4. Effect of 60 min exposure in water suspensions to Ag NPs, bulk Ag, and Ag ions (mg/L) on the culturability of PcO6 (initial cell concentration = 10^8 cfu/mL). Colonies were counted on LB agar (lacking NaCl) after 24 h for the control, and Ag treatments ≤ 1 mg/L and 36 h for treatments > 1 mg/L. Data are the means and standard deviations of 3 different studies. Error bars for some data points were too small to be visible.

To further explore the potential role of ROS, three scavengers were used to determine how they affected cell culturability. Control studies verified that none of the scavengers alone affected culturability of the cells. CAT eliminated, and SOD decreased loss in culturability caused by treatments with 1.5 mg/L Ag NPs and Ag ions. Methanol, a scavenger for hydroxyl radicals, had no protective effect (Fig. 6C). No protection occurred with the heat-denatured enzymes.

3.6. Evaluation of cell membrane integrity in the presence of Ag NP and Ag ion

Data shown in Fig. 7A confirmed that EDTA treatment of PcO6 cells ruptured the outer membrane to release the periplasmic enzyme, Alp. Exposure of cells to Ag NPs or Ag ions did not result in Alp release until the cells were treated with EDTA. The Alp levels detected after EDTA treatment of the Ag-exposed cells were significantly lower than those from control cells (Fig. 7A). Preformed Alp only showed limited inhibition by Ag NPs (3.6%) or Ag ions (7.9%).

GFP-labeled PcO6 cells were used to assess cytoplasmic membrane leakage. GFP was released when cells were ruptured following lysozyme treatment. Exposure to Ag NPs did not cause GFP leakage from the cells. Fluorescence in the cell supernatant was 6.9 ± 0.1 fluorescent units (FUs) in the cells treated with Ag NPs compared to 664 ± 6.0 FUs after lysozyme treatment. Cell supernatants from GFP cells without any treatments had 10.8 ± 0.1 FUs.

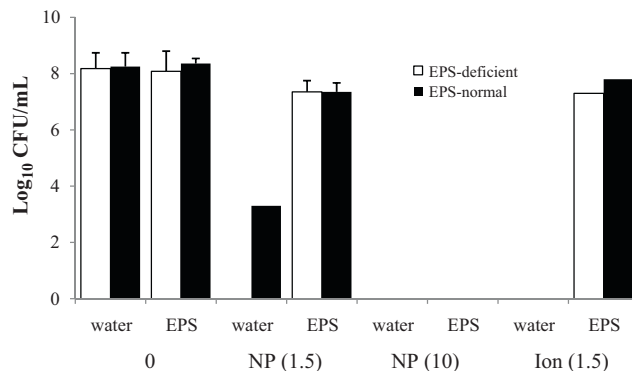


Fig. 5. Effect of EPS on the culturability of EPS-deficient and EPS-containing PcO6 cells in the presence of Ag NPs and Ag ions (in mg/L). The EPS was used at 0.81 g glucose equivalents/L. Bars represent replicates of at least 2 different experiments, each with 3 replicates. Error bars for some data points were too small to be visible.

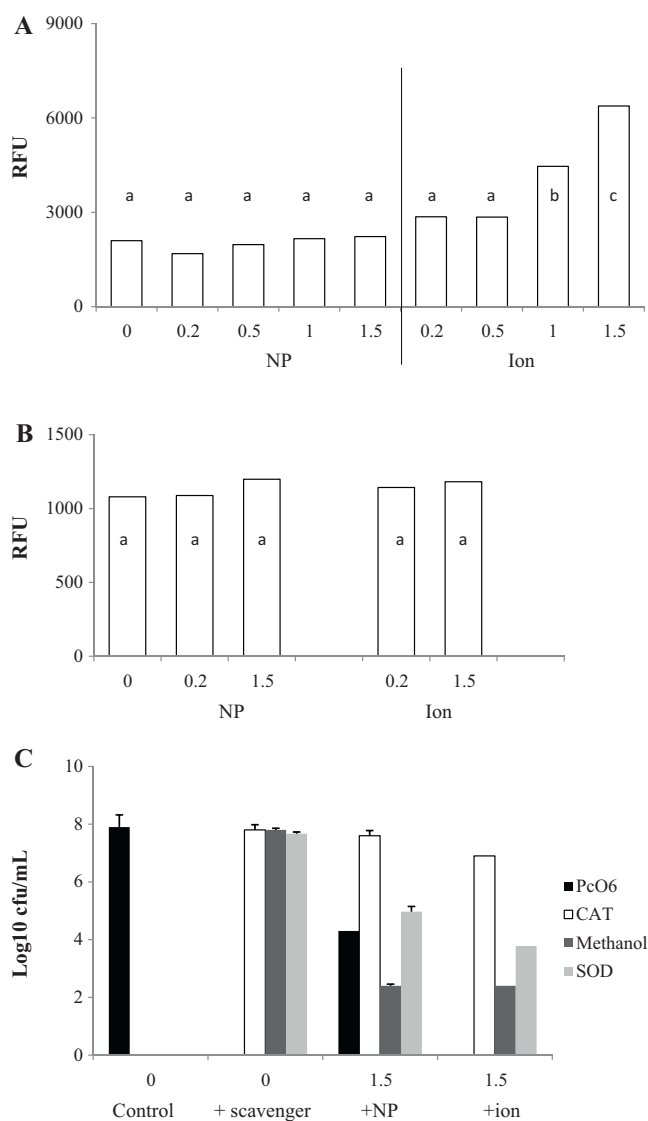


Fig. 6. Effect of Ag NPs and Ag ions (in mg/L) on the production of intracellular ROS in water-based cell suspensions of *PcO6* using (A) APF and (B) H₂-DCFDA for detection. RFU = relative fluorescent units. (C) Effect of ROS-scavenging enzymes, CAT and SOD, and the hydroxyl radical scavenger, methanol on the culturability of *PcO6*. *PcO6* cells were treated with Ag NPs and Ag ions (in mg/L) for 60 min. Culturability was measured after 48 h incubation at 28 °C on LB plates. All data are the means and SDs of 3 replicated studies and, where indicated, different letters on bars denote significant differences at $P < 0.05$. Error bars for some data points were too small to be visible.

Fluorescence microscopy images are shown in Fig. 7B. Light imaging of the fluorescent cells showed no difference in appearance for the control cells and those treated with Ag NPs. After lysozyme treatments only few intact cells with the disrupted shape of spheroplasts were visible (Fig. 7B).

4. Discussion

Imaging by AFM, as well as FFF analysis, confirmed the presence of 10 nm NPs but also showed the formation of aggregates. This mixture of differently sized particles was antimicrobial in a dose-dependent manner to the environmental isolate, *P. chlororaphis* O6. Toxicity findings were similar to those with another root-colonizing pseudomonad, *P. putida* KT2440 [4]. Sizing of the particles in the NP-preparation was important because bulk Ag at 10 mg/L did not reduce *PcO6* culturability whereas 3 mg/L Ag NPs

eliminate growth. Solubility studies showed that this preparation of Ag NPs at 10 mg/L released between 0.28 and 2.3 mg/L Ag at pH 6 and 7, whereas solubility of bulk Ag was below detection limit. Navarro et al. [32] determined using a Ag ion selective electrode, diffusive gradient thin film and ultracentrifugation that 1% of the NPs was present in solution as Ag⁺ at pH 7.5. Likewise Fabrega et al. [3] stated that less than 2% of Ag NPs would be solubilized over a pH range of 6–9. Both research groups used stabilized NPs. In this study, no stabilizers were used and the measured concentration of Ag ions was 2% at pH 6 and 20% at pH 7 of the 10 mg/L NP. Solubility was measured in deionized water with the addition of NaOH to adjust the pH to 7. The addition of base may have increased solubility of the NPs if the silver ion was complexed with hydroxide. Others have observed greater solubility of Ag NPs at pH 7.5 than pH 6 [3].

We conclude that release of ions contributed but did not account fully for the antimicrobial effect of the Ag NPs. The bacteriostasis observed with sublethal levels of both NPs and ions suggested that the cells were adjusting to the Ag challenges. Lag in growth upon exposure to Ag NPs also was observed with other bacteria [33]. Previous studies have shown that toxic levels vary depending on strain and assay conditions. For example, citrate-coated Ag NPs reduced growth of *P. fluorescens* SBW25 by 50% at 2 mg/L in the absence of a surface-coating of humic acid at alkaline pH [3] whereas *P. putida* OUS 82 *P* showed no dose-dependent toxicity to citrate-coated Ag NPs. Additionally, a toxic dose reported for *P. aeruginosa* was as high as 25 mg/L [11].

The negative charge for the Ag NP preparation agreed with prior studies, with the actual value varying depending on the different surface chemistries and media [34–36]. A higher negative ζ -potential is proposed to maintain NP stability, and hence a greater antibacterial efficacy [34,36,37]. The trend for reduction in negative charge on cells treated with Ag NPs at pH 7, but not pH 6, could reflect the extent of ion release at the two pH values.

The EPS isolated from the *PcO6* cells had a range of particle size, as determined by AFM and FFF analyses, and the surface charge was negative and similar to that of the cells; like the cells, the EPS particles did not show reduction in negative charge with Ag NPs. The cells' EPS layer protected against toxicity from challenge with both Ag ions and NPs. Our findings agreed with studies by Liu et al. [22] in concluding that EPS in a biofilm generated from uncharacterized microbes conferred protection against nitrogen-doped metal oxide NPs. With *PcO6* cells, a threshold for protection existed because 10 mg/L doses of Ag NPs remained toxic, even with additional EPS present. Different theories are proposed for EPS protection. Neal [18] suggested that the net negative charge of EPS would repulse negatively charged NPs. Also EPS may quench ROS generated by the Ag treatments [18], or it may bind the ions released from the NPs [38,39], thus, reducing cellular contact levels.

Methods used to correlate ROS production with antimicrobial activity of ions and NPs vary, and different conclusions have been drawn [7,12,23–27,40]. Using bioluminescent *Escherichia coli* cells, Huang et al. [41] observed Ag NPs differentially changed the promoter activities for genes responsive to different stresses. Using 10 nm-sized Ag NPs, they observed activation of the promoter for *sodA* (SOD) gene, supporting superoxide anion generation. They concluded that no hydrogen peroxide (H₂O₂) was involved because the promoter activity for the *katG* gene encoding CAT was not increased [24]. Our studies with *PcO6* using APF and H₂-DCFDA did not support accumulation of intracellular hydroxyl radicals from Ag NPs treatments that reduced culturability from 10⁸ to 10⁴ cells/mL. However, at the equivalent sublethal dose of ions (1 mg/L) there was enhanced APF fluorescence and response increased at 1.5 mg/L ions. The finding that the Ag ion response in fluorescence with APF was not confirmed with H₂-DCFDA could be related to the generation of other radicals, such as ⁻OCl, for which H₂-DCFDA is

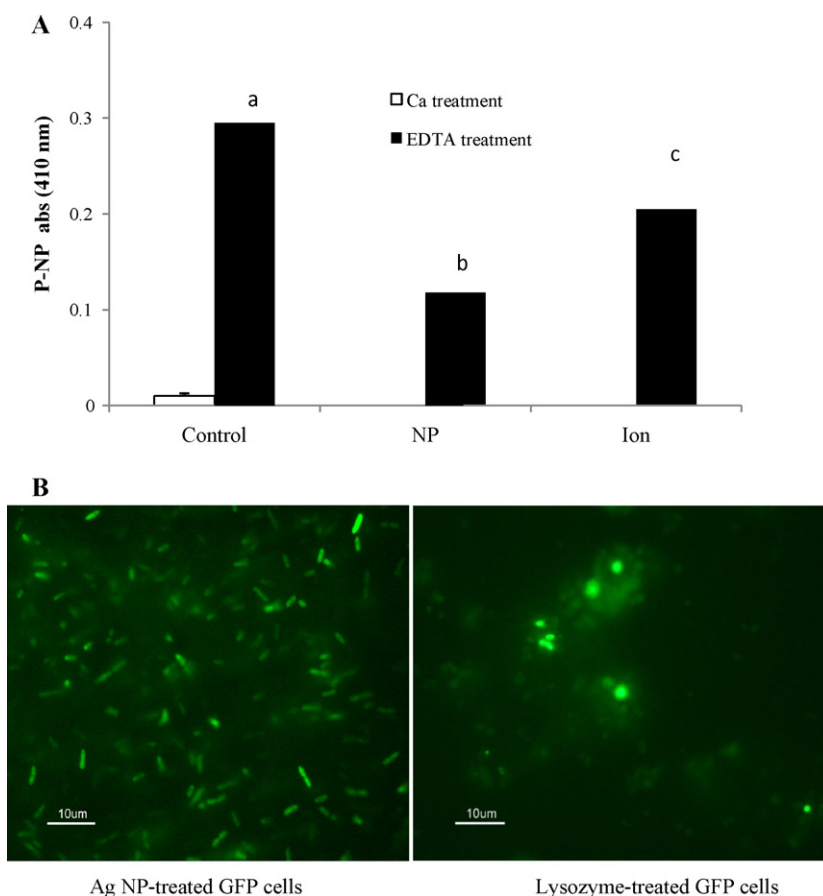


Fig. 7. Effect of Ag NPs and ions on the release of alkaline phosphatase from *Pc06*. Cells were pretreated with Ag NPs and ions (10 mg/L) for 60 min prior to treatment with Ca or with Ca followed by EDTA. (A) Alkaline phosphatase activity in supernatants from *Pc06* cells treated with Ca or EDTA, with and without exposure to Ag NPs or ions. Bars represent average absorbance (abs) at 410 nm indicating release of phosphate from the substrate, P-NPP. Letters on the EDTA treatment bars indicate significant differences ($P < 0.05$). (B) Fluorescence microscopy of GFP-transformed *Pseudomonas chlororaphis* O6 cells treated with Ag NP (left) and the effect of lysozyme demonstrating cellular lysis of transformed cells (right); some of the surviving cells are spheroplasts.

less sensitive than APF (Invitrogen). Ag ions have been shown to increase ROS in other systems. [24,26,42]. Our results from the use of scavenging enzymes and methanol provided additional knowledge. The strong protection provided by CAT, and to a lesser extent SOD, after treatments with Ag NPs suggested that both H_2O_2 and superoxide anions ($\bullet O_2^-$) were generated extracellularly. H_2O_2 is considered the most stable of the ROS [42] and such stability would allow adequate time to cause cell damage.

Other intracellular mechanisms of Ag NP toxicity independent of ROS generation also are reported to be involved in NP cytotoxicity. For example, microscopy has revealed Ag NPs within the bacterial cell cytoplasm [11,19] and cytoplasmic Ag NPs were reported to bind to DNA, impairing DNA replication and causing killing by a ROS-independent mechanism [43]. An impact at the DNA level would be consistent with the bacteriostasis that we observed with cells exposed to sublethal levels of Ag NPs.

Our analysis showing that treatments by Ag NPs did not promote a major release of periplasmic or cytoplasmic marker proteins (Alp and GFP, respectively) suggested that the NPs did not cause extensive damage to the integrity of either the inner or the outer membrane of *Pc06* cells. This assumption was supported by the report of Gou et al. [16], indicating that Ag NPs affected electron transport rather than cell membrane permeability. Aberrant electron transfer would be consistent with the modest levels of ROS that we detected. Physical damage to membranes may be minimal in our studies because of the spherical shape of the Ag NPs. Other methods of NP generation produce particles of different shapes and roughness; triangle-shaped NPs have been reported to

show stronger biocidal activity than spherical ones [10]. Membrane effects at the ultrastructure level are reported; indeed Shrivastava et al. [33] observed that Ag NPs perforated the cell membranes of *E. coli*. They also observed changes in the phosphorylated state of a tyrosine protein kinase, which are membrane associated, suggesting that the NPs altered cell signaling and, hence, cellular function.

In conclusion, we demonstrated that commercial Ag NPs were detrimental in a dose-dependent manner to the growth of a plant-beneficial soil bacterium *P. chlororaphis* O6. Toxicity occurred in spite of agglomeration of individual NPs. Such agglomerates released Ag ions at levels above that from bulk Ag materials. Toxicity could be explained in part by ion release. Ag NPs above a certain threshold circumvented the protection conferred by the EPS layer. Our findings correlated the loss in cell culturability caused by Ag NPs with production of extracellular ROS. Thus, although the antimicrobial activity of Ag NPs hold a strong promise for addressing the problem of antibiotic resistance by pathogenic bacteria, contamination of the environment by these NPs may impair the function of environmentally beneficial microbes.

Acknowledgments

This work was supported by the USDA-CSREES grant 2009-35603-05037, the Utah Agricultural Experiment Station (Journal Paper Number 8223), and the Utah Water Research Laboratory. We appreciate the lab assistance provided by Moon Jiun Ngooi and wish to thank Bill Neidermeyer for the ATTOSTAT Ag NP TEM image.

References

- [1] S.J. Klaine, P.J.J. Alvarez, G.E. Batley, T.F. Fernandes, R.D. Handy, D.Y. Lyon, S. Mahendra, M.J. McLaughlin, J.R. Lead, Nanomaterials in the environment: behavior, fate, bioavailability, and effects, *Environ. Toxicol. Chem.* 27 (2008) 1825–1851.
- [2] N. Savage, M.S. Diallo, Nanomaterials and water purification: opportunities and challenges, *J. Nanopart. Res.* 7 (2005) 331–342.
- [3] J. Fabrega, S.R. Fawcett, J.C. Renshaw, J.R. Lead, Silver nanoparticle impact on bacterial growth: effect of pH, concentration, and organic matter, *Environ. Sci. Technol.* 43 (2009) 7285–7290.
- [4] P. Gajjar, B. Pettee, D. Britt, W. Huang, W.P. Johnson, A.J. Anderson, Antimicrobial activities of commercial nanoparticles against an environmental soil microbe, *Pseudomonas putida* KT2440, *J. Biol. Eng.* 3 (2009) 9.
- [5] L. Shang, B.J. Li, W.J. Dong, B.Y. Chen, C.R. Li, W.H. Tang, G. Wang, J. Wu, Y.B. Ying, Heteronanostructure of Ag particle on titanate nanowire membrane with enhanced photocatalytic properties and bactericidal activities, *J. Hazard. Mater.* 178 (2010) 1109–1114.
- [6] A.K. Suresh, D.A. Pelletier, W. Wang, J.W. Moon, B.H. Gu, N.P. Mortensen, D.P. Allison, D.C. Joy, T.J. Phelps, M.J. Doktycz, Silver nanocrystallites: biofabrication using *Shewanella oneidensis*, and an evaluation of their comparative toxicity on Gram-negative and Gram-positive bacteria, *Environ. Sci. Technol.* 44 (2010) 5210–5215.
- [7] O. Choi, Z.Q. Hu, Size dependent and reactive oxygen species related nanosilver toxicity to nitrifying bacteria, *Environ. Sci. Technol.* 42 (2008) 4583–4588.
- [8] O. Choi, K.K. Deng, N.J. Kim, L. Ross, R.Y. Surampalli, Z.Q. Hu, The inhibitory effects of silver nanoparticles, silver ions, and silver chloride colloids on microbial growth, *Water Res.* 42 (2008) 3066–3074.
- [9] W. Su, S.S. Wei, S.Q. Hu, J.X. Tang, Preparation of TiO₂/Ag colloids with ultraviolet resistance and antibacterial property using short chain polyethylene glycol, *J. Hazard. Mater.* 172 (2009) 716–720.
- [10] S. Pal, Y.K. Tak, J.M. Song, Does the antibacterial activity of silver nanoparticles depend on the shape of the nanoparticle? A study of the gram-negative bacterium *Escherichia coli*, *Appl. Environ. Microbiol.* 73 (2007) 1712–1720.
- [11] J.R. Morones, J.L. Elechiguerra, A. Camacho, K. Holt, J.B. Kouri, J.T. Ramirez, M.J. Yacaman, The bactericidal effect of silver nanoparticles, *Nanotechnology* 16 (2005) 2346–2353.
- [12] Q.Y. Chang, H. He, Z.C. Ma, Efficient disinfection of *Escherichia coli* in water by silver-loaded alumina, *J. Inorg. Biochem.* 102 (2008) 1736–1742.
- [13] M. Gladitz, S. Reinemann, H.-J. Radusch, Preparation of silver nanoparticle dispersions via a dendritic-polymer template approach and their use for antibacterial surface treatment, *Macromol. Mater. Eng.* 294 (2009) 178–189.
- [14] M.Z. Kassae, A. Akhavan, N. Sheikh, A. Sodagar, Antibacterial effects of a new dental acrylic resin containing silver nanoparticles, *J. Appl. Polym. Sci.* 110 (2008) 1699–1703.
- [15] G.A. Sotiriou, S.E. Pratsinis, Antibacterial activity of nanosilver ions and particles, *Environ. Sci. Technol.* 44 (2010) 5649–5654.
- [16] N. Gou, A. Onnis-Hayden, A.Z. Gu, Mechanistic toxicity assessment of nanomaterials by whole-cell-array stress genes expression analysis, *Environ. Sci. Technol.* 44 (2010) 5964–5970.
- [17] C.N. Lok, C.M. Ho, R. Chen, Q.Y. He, W.Y. Yu, H.Z. Sun, P.K.H. Tam, J.F. Chiu, C.M. Che, Proteomic analysis of the mode of antibacterial action of silver nanoparticles, *J. Proteome Res.* 5 (2006) 916–924.
- [18] A.L. Neal, What can be inferred from bacterium–nanoparticle interactions about the potential consequences of environmental exposure to nanoparticles? *Eco-toxicology* 17 (2008) 362–371.
- [19] J. Fabrega, J.C. Renshaw, J.R. Lead, Interactions of silver nanoparticles with *Pseudomonas putida* biofilms, *Environ. Sci. Technol.* 43 (2009) 9004–9009.
- [20] S.M. Cho, B.R. Kang, S.H. Han, A.J. Anderson, J.Y. Park, Y.H. Lee, B.H. Cho, K.Y. Yang, C.M. Ryu, Y.C. Kim, 2R,3R-butenediol, a bacterial volatile produced by *Pseudomonas chlororaphis* O6, is involved in induction of systemic tolerance to drought in *Arabidopsis thaliana*, *Mol. Plant Microbe Interact.* 21 (2008) 1067–1075.
- [21] C.M. Ryu, B.R. Kang, S.H. Han, S.M. Cho, J.W. Kloepper, A.J. Anderson, Y.C. Kim, Tobacco cultivars vary in induction of systemic resistance against Cucumber mosaic virus and growth promotion by *Pseudomonas chlororaphis* O6 and its *gacS* mutant, *Eur. J. Plant Pathol.* 119 (2007) 383–390.
- [22] Y. Liu, C.H. Yang, J. Li, Influence of extracellular polymeric substances on *Pseudomonas aeruginosa* transport and deposition profiles in porous media, *Environ. Sci. Technol.* 41 (2007) 198–205.
- [23] Q.Y. Chang, L.Z. Yan, M.X. Chen, H. He, J.H. Qu, Bactericidal mechanism of Ag/Al₂O₃ against *Escherichia coli*, *Langmuir* 23 (2007) 11197–11199.
- [24] Y. Inoue, M. Hoshino, H. Takahashi, T. Noguchi, T. Murata, Y. Kanzaki, H. Hamashima, M. Sasatsu, Bactericidal activity of Ag-zeolite mediated by reactive oxygen species under aerated conditions, *J. Inorg. Biochem.* 92 (2002) 37–42.
- [25] J.S. Kim, E. Kuk, K.N. Yu, J.H. Kim, S.J. Park, H.J. Lee, S.H. Kim, Y.K. Park, Y.H. Park, C.Y. Hwang, Y.K. Kim, Y.S. Lee, D.H. Jeong, M.H. Cho, Antimicrobial effects of silver nanoparticles, *Nanomed. Nanotechnol. Biol. Med.* 3 (2007) 95–101.
- [26] H.J. Park, J.Y. Kim, J. Kim, J.H. Lee, J.S. Hahn, M.B. Gu, J. Yoon, Silver-ion-mediated reactive oxygen species generation affecting bactericidal activity, *Water Res.* 43 (2009) 1027–1032.
- [27] M. Cho, H. Chung, W. Choi, J. Yoon, Different inactivation behaviors of MS-2 Phage and *Escherichia coli* in TiO₂ photocatalytic disinfection, *Appl. Environ. Microbiol.* 71 (2005) 270–275.
- [28] M.I. Torino, M.P. Toranto, F. Sesma, G. Font de Valdez, Heterofermentative pattern and exopolysaccharide production by *Lactobacillus helveticus* ATCC 15807 in response to environmental pH, *J. Appl. Microbiol.* 91 (2001) 846–852.
- [29] M.W. Pabst, A.J. Anderson, C.D. Miller, C. Dimkpa, J.E. McLean, Defining the surface adsorption and internalization of copper and cadmium in a soil bacterium, *Pseudomonas putida*, *Chemosphere* 81 (2010) 904–910.
- [30] G. Guang, Z. Guanwei, Q. Boqiang, C. Jun, W. Ke, Alkaline phosphatase activity and the phosphorus mineralization rate of Lake Taihu, *Sci. China: Series D Earth Sci.* 49 (2006) 176–185.
- [31] Y.C. Kim, C.D. Miller, A.J. Anderson, Superoxide dismutase activity in *Pseudomonas putida* affects utilization of sugars and growth on root surfaces, *Appl. Environ. Microbiol.* 66 (2000) 1460–1467.
- [32] E. Navarro, F. Piccapietra, B. Wagner, F. Marconi, R. Kaegi, N. Odzak, L. Sigg, R. Behra, Toxicity of silver nanoparticles to *Chlamydomonas reinhardtii*, *Environ. Sci. Technol.* 42 (2008) 8959–8964.
- [33] S. Shrivastava, T. Bera, A. Roy, G. Singh, P. Ramachandrarao, D. Dash, Characterization of enhanced antibacterial effects of novel silver nanoparticles, *Nanotechnology* 18 (2007) 225103.
- [34] R. Barrena, E. Casals, J. Colon, X. Font, A. Sanchez, V. Puentes, Evaluation of the ecotoxicity of model nanoparticles, *Chemosphere* 75 (2009) 850–857.
- [35] A. Dror-Ehre, H. Mamane, T. Belenkova, G. Markovich, A. Adin, Silver nanoparticle–*E. coli* interaction in water and effect on *E. coli* survival, *J. Colloid Interface Sci.* 339 (2009) 521–526.
- [36] A.M. El-badawy, T.P. Luxton, R.G. Silva, K.G. Scheckel, M.T. Suidan, T.M. Tolaymat, Impact of environmental conditions (pH, ionic strength, and electrolyte type) on the surface charge and aggregation of silver nanoparticles suspensions, *Environ. Sci. Technol.* 44 (2010) 1260–1266.
- [37] W.-L. Du, S.-S. Niu, Y.-L. Xu, Z.-R. Xu, C.-L. Fan, Antibacterial activity of chitosan tripolyphosphate nanoparticles loaded with various metal ions, *Carbohydr. Polym.* 75 (2009) 385–389.
- [38] J.W. Moreau, P.K. Weber, M.C. Martin, B. Gilbert, I.D. Hutcheon, J.F. Banfield, Extracellular proteins limit the dispersal of biogenic nanoparticles, *Science* 316 (2007) 1600–1603.
- [39] J.A. Rojas-Chapana, H. Tributsch, Interfacial activity and leaching patterns of *Leptospirillum ferrooxidans* on pyrite, *FEMS Microbiol. Ecol.* 47 (2004) 19–29.
- [40] D.B. Hamal, J.A. Haggstrom, G.L. Marchin, M.A. Ikenberry, K. Hohn, K.J. Klabunde, A multifunctional biocide/sporicide and photocatalyst based on titanium dioxide (TiO₂) codoped with silver, carbon, and sulfur, *Langmuir* 2 (2010) 2805–2810.
- [41] Z.B. Huang, X. Zheng, D.H. Yan, G.F. Yin, X.M. Liao, Y.Q. Kang, Y.D. Yao, D. Huang, B.Q. Hao, Toxicological effect of ZnO nanoparticles based on bacteria, *Langmuir* 24 (2008) 4140–4144.
- [42] R. Pedahzur, O. Lev, B. Fattal, H.I. Shoval, The interaction of silver ions and hydrogen-peroxide in the inactivation of *Escherichia coli*—a preliminary evaluation of a new long-acting residual drinking-water disinfectant, *Water Sci. Technol.* 31 (1995) 123–129.
- [43] W. Yang, C. Shen, Q. Ji, H. An, J. Wang, Q. Liu, Z. Zhang, Food storage material silver nanoparticles interfere with DNA replication fidelity and bind with DNA, *Nanotechnology* 20 (2009) 085102.